J Cancer Res Clin Oncol (2006) 132:685–697
DOI 10.1007/s00432-006-0117-5

ORIGINAL PAPER

The membrane-cytoskeleton organizer ezrin is necessary for hepatocellular carcinoma cell growth and invasiveness

Yan Zhang · Mei-Yu Hu · Wei-Zhong Wu · Zhi-Jun Wang · Kang Zhou · Xi-Liang Zha · Kang-Da Liu

Received: 12 December 2005 / Accepted: 25 April 2006 / Published online: 20 June 2006

Abstract *Purpose* The change of cell mobility is one of the preconditions of tumor metastasis. Cell skeleton alteration and rearrangement of F-actin was closely related to cell mobility. Ezrin is a membrane-cytoskeleton organizer that can mediate the rearrangement and the function of F-actin. In this paper, we investigated the effect of ezrin on hepatocellullar carcinoma cell growth and invasiveness.
Methods Hepatocellular carcinoma cell lines such as MHCC-1, MHCC97-H, SF7721, SMMC7721, Hep3B, and HepG2 were chosen in this study. We first examined the expression and the distribution of ezrin and F-actin in these cell lines using immunofluorescence, RT–PCR, and the western blot. Next we used small interfering RNA (siRNA) to down-regulate ezrin expression in MHCC-1, MHCC97-H, SF7721, and HepG2 to investigate the role of ezrin in tumor cell growth and invasiveness.
Results Our preliminary results showed that the expression of ezrin and γ-actin in MHCC-1, MHCC97-H, and SF7721 with higher metastatic potential were obviously up-regulated than those in SMMC7721, Hep3B, and HepG2 with lower potential. No different expression of β-actin was found in the above tumor cell lines. The outcome of RNAi indicated that decreasing ezrin expression can notably inhibit the proliferation of the four hepatocellular carcinoma cell lines ($p < 0.01$, $n = 10$). The proportion of cells in G2-M phase also decreased after RNAi. The number of pseudopods decreased as well after RNAi treatment ($p < 0.01$, $n = 5$). The mobility and invasiveness of cancer cells decreased with decreasing ezrin expression tested by transwell assay ($p < 0.01$, $n = 8$).
Conclusion Ezrin plays an important role in the process of hepatocellular carcinoma cell proliferation, migration, and invasiveness.

Keywords Hepatocellular carcinoma · Ezrin · RNAi · Invasiveness

Introduction

Hepatocellular carcinoma is a malignant tumor with high relapse and metastasis. Despite recent improvement in long-term survival rates, its prognosis is still poor. It is necessary to find new therapeutic molecular targets to ameliorate its outcome. Disruption of actin filaments and a decrease in focal adhesion are common features \in various oncogene-transformed cells (Pawlak and Helfman 2000). Structural changes of actin filaments will alter cell mobility, which is critical to tumor metastasis. Ezrin is a 81-kDa protein which have been shown to perform structural and regulatory roles in the assembly and stabilization of plasma membrane domains. Ezrin and related molecules are concentrated at surface projections such as microvilli and membrane ruffles where they link the microfilaments to the mem-

Y. Zhang · M.-Y. Hu · Z.- J. Wang · K. Zhou · K.-D. Liu (✉)
Experimental Center of Zhongshan Hospital,
Fudan University, Shanghai, 200032, China
e-mail: ch_zy@hotmail.com

W.-Z. Wu
Liver Cancer Institute, Fudan University, Shanghai, China

X.-L. Zha
Department of Biochemistry and Molecular Biology,
Shanghai Medical College, Fudan University,
Shanghai, China

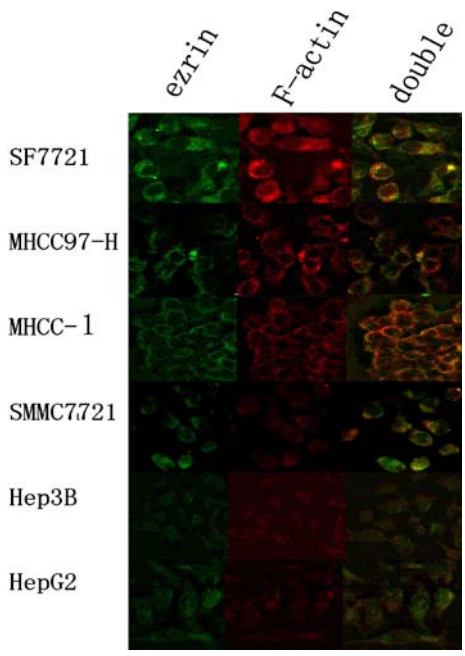

Fig. 1 Differential expression of ezrin and F-actin in different hepatocellular carcinoma cell lines. All the cell lines express ezrin and F-actin. SF7721, MHCC-1, and MHCC97-H with high metastasis potential have a higher ezrin and F-actin expression level than SMMC7721, Hep3B, and $HepG_2$ with low potential. Double color staining showed ezrin and F-actin always co-expressed in one cell with positive correlation

brane. It allows cross-linking of actin filaments and regulation of actin filaments prior to cell mobility. Ezrin protein is believed to be a membrane organizer and linker between plasma membrane molecules such as CD44 and ICAM-2 and the cytoskeleton (Yonemura et al. 1999; Sainio et al. 1997). Ezrin in cytoplasm often exists in an inactive conformation, with N-terminal to C-terminal associations within the protein or with other ezrin/radixin/moesin (ERM) family members. Upon threonine and tyrosine phosphorylation, ezrin acquires an active conformation, moves to the cell membrane, and tethers F-actin directly or indirectly to cell membrane (Bretscher et al. 2002; Nguyen et al. 2001). Some studies have implicated that ezrin protein was over-expressed in many metastatic cell lines, as it has been found to be over-expressed in invasion of endometrial cancer cells (Ohtani et al. 1999). High expression of ezrin in many cultured cells causes cell transformation and is associated with cell proliferation (Kaul et al. 1996). But its role in the process of hepatocellular carcinoma growth and metastasis has not been defined.

To study the role of ezrin in hepatocellular carcinoma cells, we explored the differential expression of ezrin and F-actin in hepatocellular carcinoma cell lines with different metastasis potential, and used small interfering RNA (siRNA) to down-regulate the ezrin expression to observe the changes of tumor cell growth and invasiveness. Functional analyses revealed that the abrogation of ezrin strongly inhibits proliferation, migration, and invasiveness of hepatocellular carcinoma. We concluded that ezrin was a critical molecule in hepatocellular carcinoma growth migration and invasiveness.

Materials and methods

Cell lines

Six hepatocellular carcinoma cell lines were chosen in this study. SF7721 (SMMC7721 stably transfected with human HGF/SF) (Xie et al. 2001), MHCC-1 (metastatic hepatocellular carcinoma cell line), and MHCC97-H are the cell lines with high metastasis potential. SMMC7721, Hep3B, and HepG2 are the cell lines with low metastasis potential. SF7721 was grown in DMEM (Invitrogen) with 10% heat-inactivated fetal bovine serum (HyClone, Logan, UT) and 400 μg/mlG418; MHCC-1 and MHCC97-H were grown in DMEM (Invitrogen) with 10% human AB serum.

Table 1 The cell percentage of ezrin in five intensity degree of different cell lines

Cell lines	Cell percentage of various fluorescent intensity[a]					Cell percentage of various fluorescent intensity[b]				
	++++	+++	++	+	−	++++	+++	++	+	−
SF7721	80	12	4	3	1	85	10	2	3	0
MHCC-1	75	12	8	4	1	82	12	3	3	0
MHCC97-H	73	10	8	9	3	79	14	4	3	0
SMMC7721	21	31	24	20	4	46	20	24	10	0
Hep3B	23	20	30	25	2	43	22	20	15	0
HepG2	19	23	28	28	2	35	20	29	16	0

The strongest intensity is 100; ++++ ranges from 75 to 100; +++ ranges 50 to 75; ++ ranges from 25 to 50; + ranges from 25 to 50 and the intensity is 0 in −

[a] $X^2 = 13.277$, $p = 0.010$

[b] $X^2 = 21.815$, $p = 0.000$

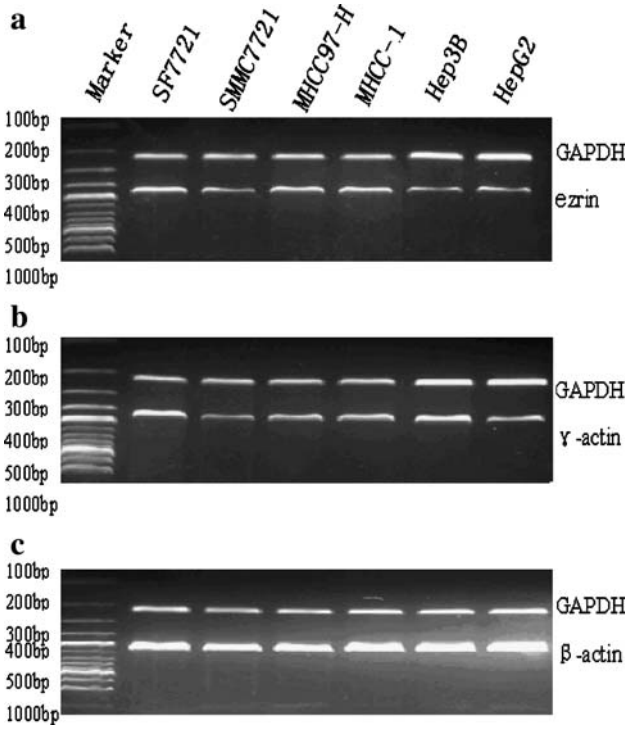

Fig. 2 Expression of ezrin and actin mRNA in different cell lines. **a** The expression of ezrin mRNA in cell lines with high metastasis potential SF7721, MHCC-1, MHCC97-H, and MHCC97-L was significantly higher than that in SMMC7721, Hep3B, and $HepG_2$ with low potential. **b** γ-Actin also has a stronger expression in cell lines with higher metastasis potential than those with lower metastasis potential. **c** β-Actin mRNA has no expression difference in cell lines with different metastasis potential

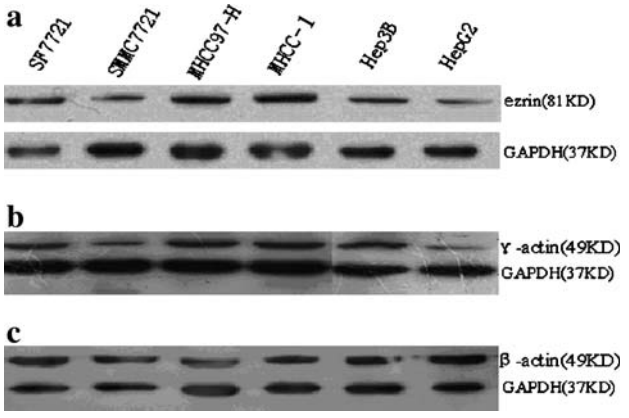

Fig. 3 Differential expression of ezrin and actin protein in different cell lines. Western blot showed (**a**) the expression of ezrin in cell lines with high metastasis potential SF7721, MHCC-1, and MHCC97-H was significantly stronger than that in SMMC7721, Hep3B, and $HepG_2$ with low potential. **b**. γ-Actin also has a stronger expression in cell lines with higher metastasis potential than those with lower metastasis potential. **c** β-Actin has no expression deference in cell lines with deferent metastasis potential

SMMC7721, Hep3B, and HepG2 were grown in DMEM (Invitrogen) with 10% heat-inactivated fetal bovine serum (HyClone, Logan, UT). Ezrin and F-actin expressions were detected in all the cell lines. SF7721, MHCC-1, MHCC97-H, and HepG2 were selected to do RNA interference.

Immunofluorescence

Autoclaved coverslips were placed into 3.5-mm culture dishes. Approximately, 1×10^5 cancer cells were seeded into each dish after adding 2 ml of culture media. The cells were cultured for more than 24 h until they reach 40–50% confluent. Drawing off culture media and rinsing the dish with warm PBS for three times. Five drops of paraformaldehyde were added into dishes for 30 min at room temperature. Fifty microliters of 1% Triton in PBS was added for 30 min to enhance the membrane permeability. Hundred microliters of human anti-Rabbit ezrin 1:100 (Upstate Corporation) and human anti-Mouse F-actin 1:10 (Serotec Corporation) mixture was incubated with cells in 4 °C, overnight. The second antibody mixture was prepared by rhodamine-labeled sheep anti-rabbit antibody (1:100) and FITC-labeled horse anti-mouse antibody (1:100) and incubated with cells at room temperature for 1 h. The coverslips were sealed by 50% glycerol in PBS and observed under fluorescent microscope.

Reverse transcription-PCR analysis

Total RNA was isolated with TRIzol reagent (Invitrogen). Reverse transcription was done with 1 g RNA and the SuperScript II RNase H-Reverse Transcriptase (Invitrogen), and with 1 μl Transcriptase (Invitrogen).

Table 2 siRNA sequence specific to ezrin

siRNA number	19-mer target sequence
Ezrin-siRNA1	5′-AUCAGGUGGUAAAGACUAUdtdt-3′ (sense); 5′-AUAGUCUUUACCACCUGAUdtdt-3′ (antisense)
Ezrin-siRNA2	5′-ACUUUGGCCUCCACUAUGUdtdt-3′ (sense); 5′-ACAUAGUGGAGGCCAAAGUdtdt-3′ (antisense)
Ezrin-siRNA3	5′-CCCUUGGACUGAAUAUUUAdtdt-3′ (sense); 5′-UAAAUAUUCAGUCCAAGGGdtdt-3′ (antisense)
Ezrin-siRNA4	5′-GGCUUUCCUUGGAGUGAAAdtdt-3′ (sense); 5′-UUUCACUCCAAGGAAAGCCdtdt-3′ (antisense)
Scramble siRNA	5′-UUCUCCGAACGUGUCACGUdtdt-3′ (sense); 5′-ACGUGACACGUUCGGAGAAdtdt-3′ (antisense)

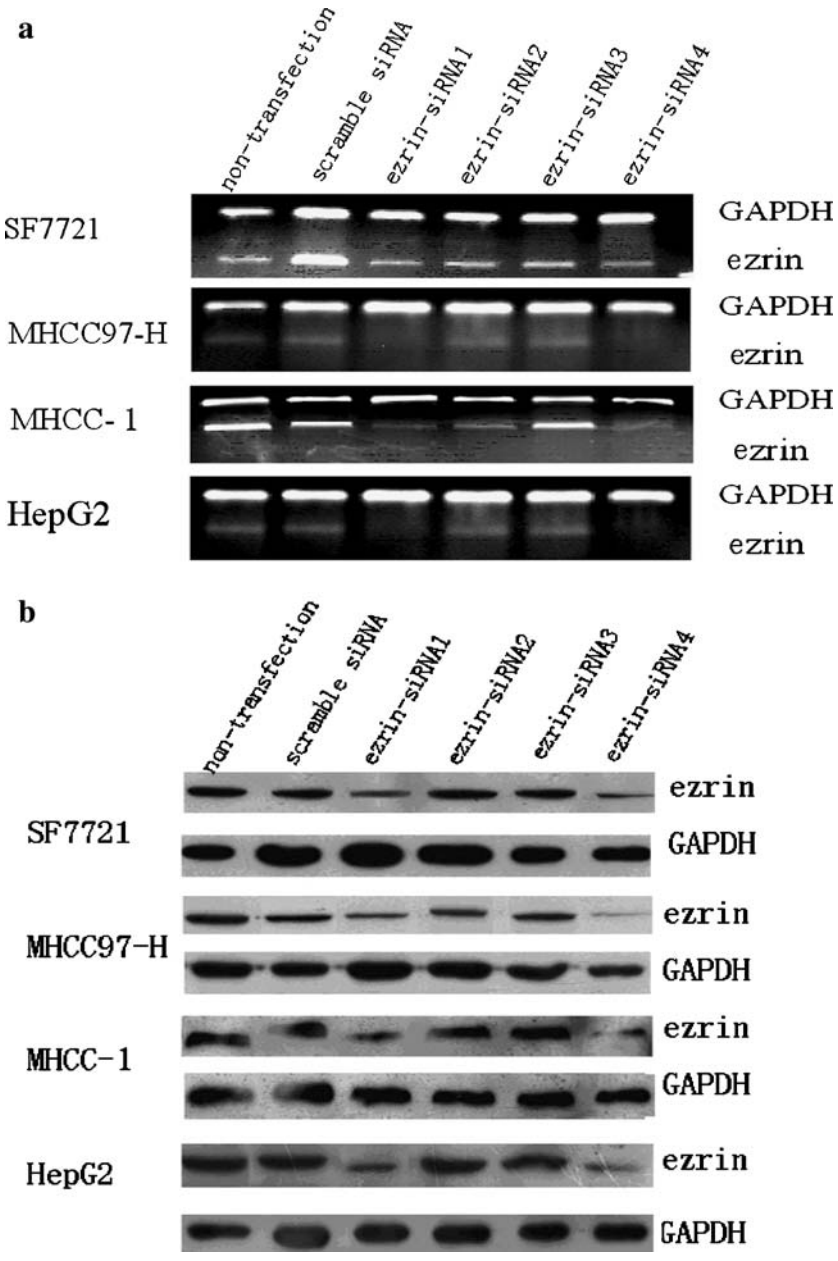

Fig. 4 Screening the most effective ezrin-siRNA. **a** RT-PCR assay showed that ezrin-siRNA1 and ezrin-siRNA4 have a higher suppression rate to ezrin mRNA in all the hepatocellular carcinoma cell lines. **b** The protein level suppression detected by western blot shows the same result with the suppression in the mRNA level. However, ezrin-siRNA4 has the best suppression effect in protein level

One reverse transcriptase product was used for amplification of ezrin, β-actin, or γ-actin genes. The primers used were as follows. Ezrin: 5′-CTCATCCAGGACA TCACCCA-3′ (sense), 5′-TCACTCCAAGGAAAG CCAAT-3′ (antisense), 450 bp; β-actin: 5′-GACAGG ATGCAGAAGGAGAT-3′ (sense), 5′-TGTGTGGA CTTGGGAGAGGACT-3′ (antisense), 550 bp; γ-actin: 5′-AAGTACCCCATTGAGCATGGC-3′ (sense), 5′-CACAGCTTCTCCTTGATGTCGC-3′ (antisense), 449 bp; GAPDH: 5 ′-GAAGGTGAAGGTCGGAG TC-3′ (sense), 5′-GAAGATGGTGATGGGATTTC-3′ (antisense), 226 bp. The PCR conditions were 95 °C for 5 min, followed by 35 cycles of 95 °C, 30 s; 55 °C, 30 s; and 72 °C, 30 s. The final extension was 72 °C for 10 min. The PCR products were run on 2% agarose and detected by gel analysis system.

Western blot analysis

Cell extracts were separated by 12% SDS–PAGE and transferred to polyvinylidene difluoride membranes (Millipore Corporation). The membranes were incubated with antibodies against ezrin (Upstate Corporation), β-actin (Abcam Corporation), γ-actin (Chemicon Corporation), and GAPDH (Chemicon Corporation), 4 °C, overnight. Then incubated with HRP-labeled second antibody at room temperature for 1 h. After incubation with ECL reagent (Amersham Biosciences,

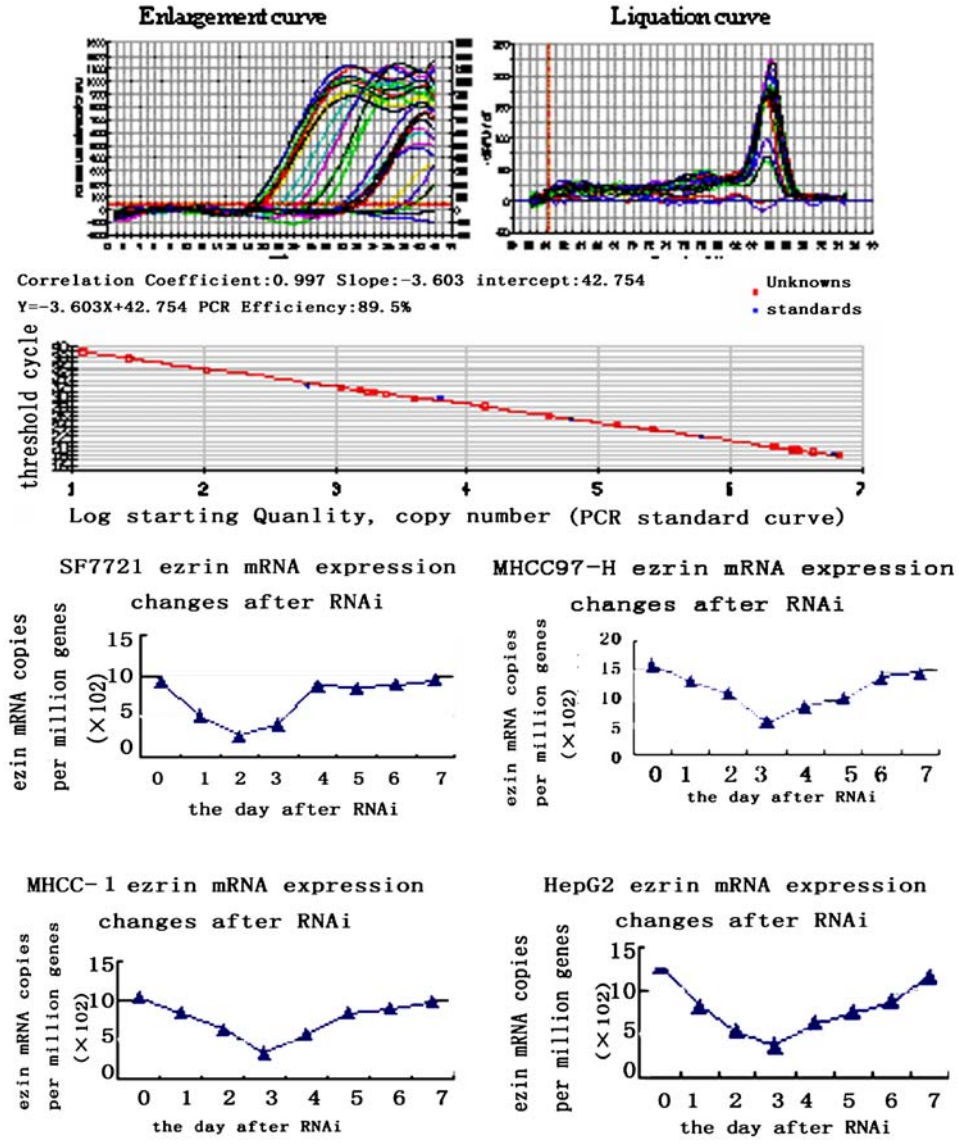

Fig. 5 The down-regulation rate of ezrin mRNA and time-course of ezrin-siRNA in four different cell lines. The down-regulation occurred in the first day after RNAi and lasted 3–4 days. The strongest down-regulation appeared in the third day after RNAi in MHCC97-H, MHCC-1, and HepG2, However, it is appeared in the second day after RNAi in SF7721. The down-regulation rate is different according to different cell lines: MHCC97-H: 64%; MHCC-1: 67%; SF7721: 72%; $HepG_2$: 72%

Buckinghamshire, UK), chemiluminescence signals were photographed and quantitated by image analysis.

siRNA transfection

Transfection of ezrin-siRNA was conducted with Lipofectamine 2000 (Invitrogen) in 6-well plates according to the manufacturer's specification. The day before transfection, the cells were trypsinized, counted, and seeded at 1×10^5 cells per well into 6-well plates, so that they were 80–90% confluence on the day of transfection. Lipofectamine 2000 diluted in opti-MEM (Invitrogen) was supplemented into the siRNA mixture. Incubate the mixture for 20 min at room temperature. The mixture and opti-MEM were added into the plate so that the terminal siRNA concentration is 125 nM. The mixture without siRNA was also transfected as control, and all the mixtures were replaced by complete DMEM after 5-h reaction.

Real-time PCR analysis

Total RNA was isolated with TRIzol reagent (Invitrogen). Reverse transcription was done with 1 μg RNA and the SuperScript II RNase H-Reverse Transcriptase (Invitrogen). Real-time PCR was performed by

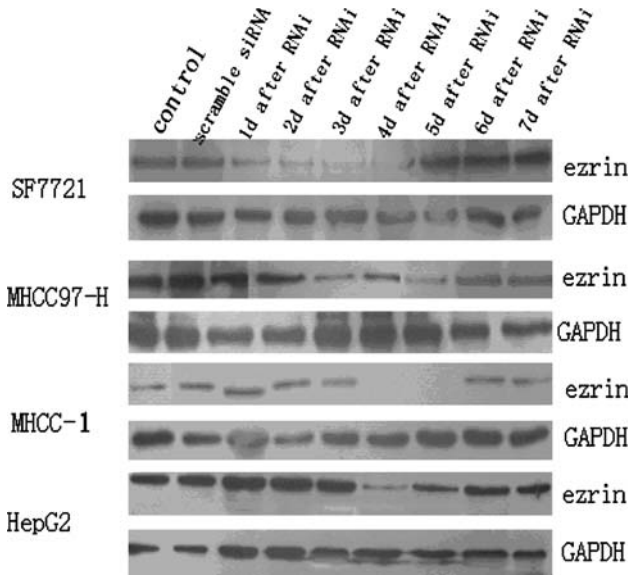

Fig. 6 Suppression rate of ezrin and time-course of ezrin-siRNA in four different cell lines. The down-regulation occurred in the first days after RNAi and lasted 4 days in SF7721. The strongest down-regulation appeared in the third and fourth days after RNAi. The down-regulation occurred in the third day after RNAi and lasted 3 days in MHCC97-H. The strongest down-regulation appeared in the fifth day after RNAi. In MHCC-1, the down-regulation occurred in the third day after RNAi and lasted 3 days. The strongest down-regulation appeared in the fourth and fifth days after RNAi. The down-regulation occurred in the fourth day after RNAi and lasted 2 days in HepG2. The strongest down-regulation appeared in the fourth day after RNAi

Real-time PCR kit (TaKaRa Corporation), and the products were labeled by SYBR Green I (BIORADC). The PCR primers for quantitative real-time PCR were ezrin: 5′-GCCGAAACCAATCAATGTC-3′ (sense), 5′-TTCAGCCAGGTAGGAAATCC-3′ (antisense), 177 bp; GAPDH: 5′-AAGGTCGGAGTCGTCAACGGATT-3′ (sense), 5′-CTGGAAGATGGTGATGGGATT-3′ (antisense), 222 bp. PCR condition was: 95 °C: 90 s; 95 °C: 5 s; 58 °C: 30 s (40 cycles); 95 °C: 1 min, 55 °C: 1 min; 55 °C: 10 s (+0.5 °C/cycle, 80 cycles).

MTT assay

Five hours after siRNA transfection, 1×10^3 (SF7771) or 2.5×10^3 (MHCC-1, MHCC97-H, and $HepG_2$)/per well were seeded into a 96-well culture plate and let the cells attach overnight. Non-transfected cells were also seeded as control. Five milligrams per milliliter MTT in PBS was prepared. Twenty hours after transfection, we remove the culture medium from the plate and add 100 μl of fresh culture medium and 20 μl of MTT solution, then incubate at 37 °C for 4 h. MTT medium mixture was removed drastically and 100 μl of DMSO was added into each well. The plates were shaken evenly for 5 min to dissolve the precipitate, and then were read at 540 nm in microplate reader. The test was repeated once a day after transfection for 10 days and the trendlines were protracted according to the OD values.

Cell cycles and apoptosis assay

Cells (1×10^5 per well) were seeded into 6-well plates and transfected with ezrin-siRNA. Cells were harvested 3 or 4 days after transfection and processed for flow cytometric analysis. The suspensions of tumor cells were prepared with the detergent-trypsin method and then were stained with propidium iodide. Measurement of DNA cellular contents was done with a FACSCalibur flowcytometer.

Electron microscope assay

Autoclaved coverslips were placed into a 3.5-mm culture dish. Two or 3 days after transfection, 1×10^5 cancer cells were seeded into each dish after adding 2 ml of culture media. Culture the cells for 24 h until they reach 60–70% confluent. The culture media were drawn off and rinsed the dish with warm PBS for three times. The cells were fixed with 2.5% glutaraldehyde and postfixed with 2% osmium tetraoxide. After full dehydration with gradient concentrations of ethanol, the samples were adhered to an aluminum stub and sprayed plating with gold for 3 min, which were further examined by HITACHI R250 electron microscope with the attachment of scanning apparatus. The pseudopods were counted under 2,000× visual field.

Transwell assay

Transwell double chambers with 8-mm pore size (Costar, Cambridge, MA) were covered with 20 μl of Matrigel by incubating for 30 min at 37 °C. Transwell chambers with reconstituted Matrigel membranes were set on 24-well cluster plates. The cells were trypsinized and counted, then resuspended with fresh medium. Approximately, 1×10^5 cells were placed in 200 μl of defined medium into upper chamber. Three hundred microliters of medium was added into lower chamber. The cell lines MHCC-1, MHCC97-H, and SF7721 were cultured for approximately 20 h. $HepG_2$ was cultured for more than 48 h because of its low metastasis potential. The medium in lower chamber was aspirated after culture and 5 ml of 4% paraformaldehyde in 1× PBS was added, incubating for 30 min at room temperature. The wells were washed by PBS after aspirating paraformaldehyde. The inner surface of the upper chamber was carefully wiped using a cotton swab. The

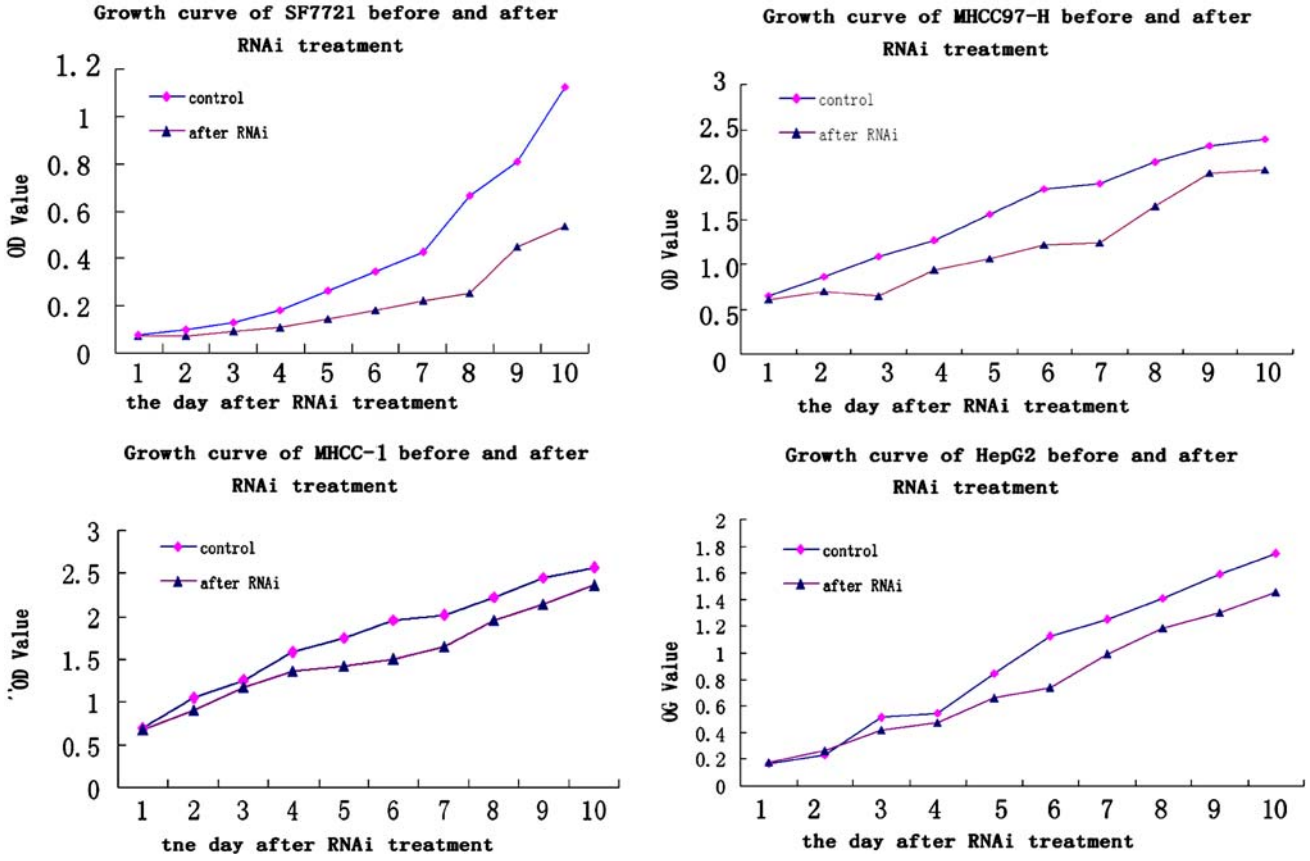

Fig. 7 Proliferation changes before and after RNAi treatment. The trendlines according to *OD* value in 10 days after RNAi showed that cell proliferation was definitely decreased after ezrin-siRNA was transfected into four different caner cell lines. It is suggested that ezrin is positively related to cancer cell growth (SF7721: $t = 3.2$; $p < 0.05$; MHCC97-H: $t = 6.297$, $p < 0.01$; $HepG_2$: $t = 3.985$; $p < 0.01$; MHCC-1: $t = 5.856$, $p < 0.01$)

membranes were stained with Giemsa and the cells were counted with q 20× objective of microscope. At least eight fields were counted per membrane.

Statistical analyses

All statistical analyses were performed using Microsoft Excel and SPSS software.

Results

Differential expression of ezrin and F-actin in various hepatocellular carcinoma cell line

We tested the expression and distribution difference of F-actin and ezrin in hepatocellular carcinoma cell lines with different metastatic potential by immunofluorescence (Fig. 1). We found that ezrin and F-actin exist in the plasma of all the cell lines. Double color staining showed that ezrin and F-actin always co-expressed in one cell with positive correlation. The fluorescence intensity was classified into five, as −, +, ++ +++, and ++++ representing the increasing intensity. The cell percentage in five intensity degree was listed in Table 1. The results suggested that high metastatic cell lines such as SF7721, MHCC-1, and MHCC97-H usually have higher expression of ezrin and F-actin than that in low metastatic cell lines as SMMC7721, Hep3B, and HepG2 ($p < 0.05$).

We also use RT-PCR to analyze the differential expression of ezrin and F-actin in mRNA level. F-actin is a polymer of α-actin, β-actin, and γ-actin; however, only β-actin and γ-actin are the cytoplasma types. So we designed primers for ezrin, β-actin, and γ-actin, respectively, to determine the difference in their expression. Ezrin and γ-actin mRNA in SF7721, MHCC-1, and MHCC97-H were significantly expressed higher than that in SMMC7721, Hep3B, and $HepG_2$ with low metastasis potential. β-Actin mRNA has no difference in the expression in cell lines with different metastasis potential (Fig. 2). Western blot gained the same results with RT-PCR in protein level. High ezrin and γ-actin protein level was correlated with high metastatic potential (Fig. 3).

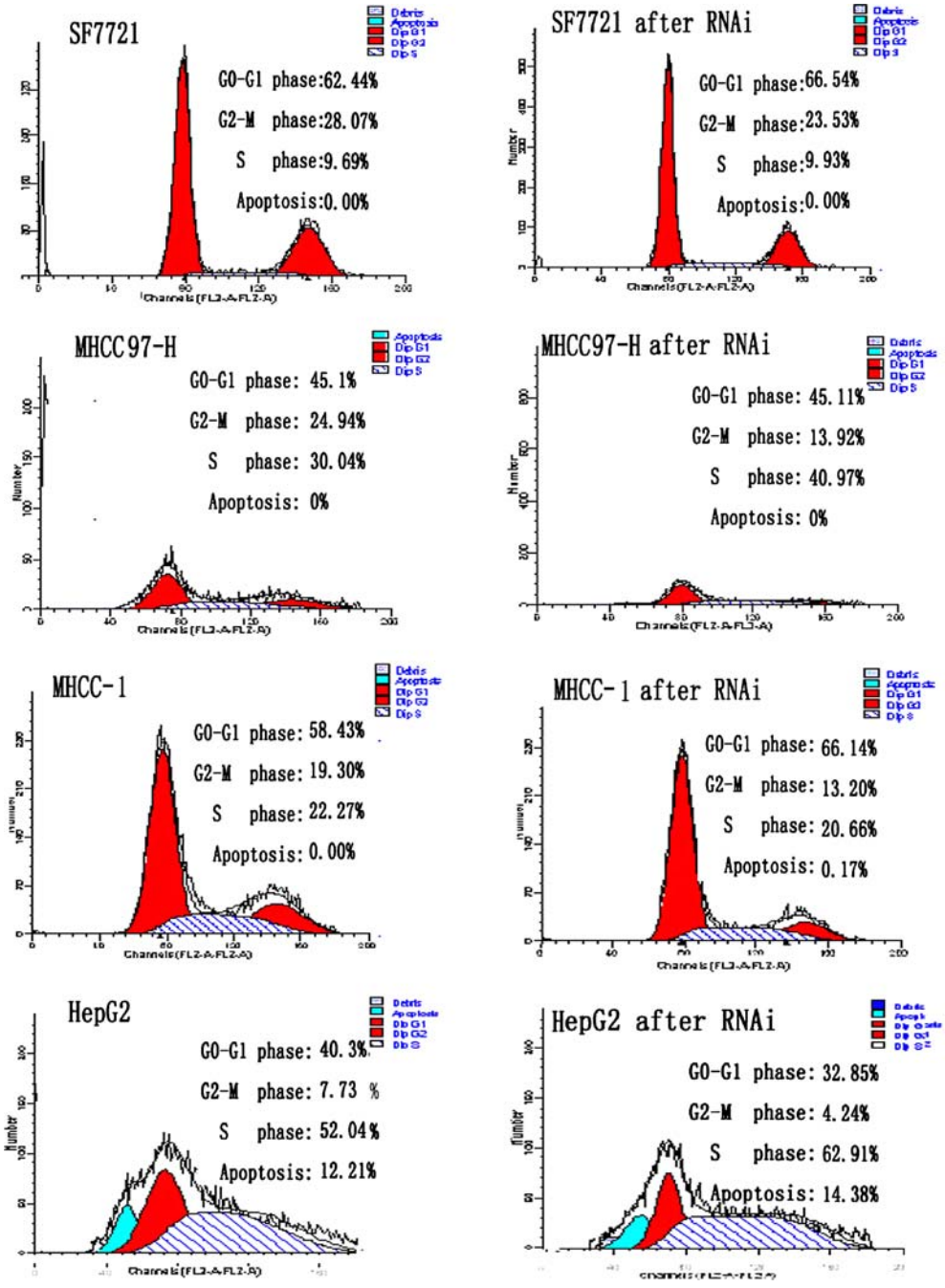

Fig. 8 Cell-cycle changes after RNAi treatment. The proportion of the cells in G2-M phase is decreased after RNAi in all cell line. The cell proportion in G2-M phase was 23.53% compared with 28.07% before RNAi in SF7721.The proportion is 13.92% compared with 24.94% before RNAi in MHCC-97H; 7.73% compared with 4.24% before RNAi in $HepG_2$. In MHCC-1, the cell proportion in G2-M phase is 13.20% compared with 19.30% before RNAi. In addition, the cells in G1 point were also increased. No apoptosis inducing effect was detected

Designing ezrin-siRNAs and transfecting them into hepatocellular carcinoma cell lines

Search full-length gene sequence of ezrin in GenBank and designed four pairs of ezrin-siRNA according to http://www.ambion.com/techlib/misc/siRNA_finder.html. All siRNA sequences synthesized by GeneChem Corporation, China, were listed in Table 2, siRNA was transfected into cells by lipofectamine 2000. Transfection efficacy was evaluated by intensity of FITC-labeled scramble siRNA under fluorescent microscopy. The siRNA transfection rates in all cell lines were more than 90%.

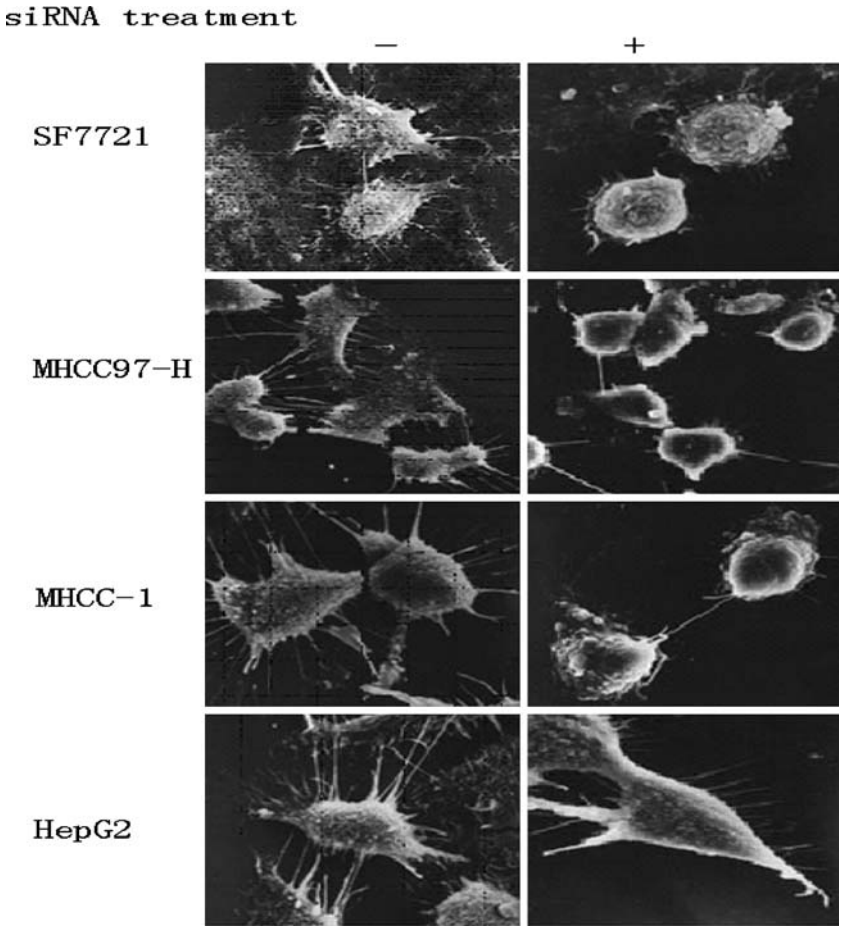

Fig. 9 Morphological changes after RNAi treatment. The pseudopods formation in all cell lines was obviously decreased compared with that before RNAi. In addition, the pseudopods after RNAi became shorter and thinner than those before RNAi (SF7721: $t = 4.95$, $p < 0.01$; MHCC97-H: $t = 5.88$, $p < 0.01$; MHCC-1: $t = 5.56$, $p < 0.01$; HepG2: $t = 5.71$, $p < 0.01$)

Screening for the effective ezrin-siRNA

RT-PCR and western blot were used to screen the most effective siRNA from four designed siRNA. RT-PCR demonstrated ezrin-siRNA1, and ezrin-siRNA4 can drastically down-regulated ezrin mRNA expression in MHCC-1, MHCC97-H, SF7721, and $HepG_2$ cell lines. Western blot gained the same results (Fig. 4), but ezrin-siRNA4 can down-regulate ezrin protein more prominently than ezrin-siRNA1. So we select ezrin-siRNA4 to do the following study.

Detection of the efficiency and time-course of ezrin-siRNA transfection to select a proper time point for the proliferation and invasiveness assay

Ezrin-siRNA4 was transfected into four hepatocellular carcinoma cell lines in a 6-well culture plate. RNA and protein were extracted every day following siRNA transfection until day 7 and the down-regulation efficacy and time-course of ezrin-siRNA were analyzed by real-time PCR and western blots. Our PCR results show that ezrin mRNA appeared to be down-regulated in first day after RNAi transfection. About 72% ezrin mRNA appeared to be down-regulated in siRNA-transfected SF7721 in the second day, whereas 64, 67, and 72% ezrin mRNA were observed to be down-regulated in siRNA-transfected MHCC97-H, MHCC-1.

Table 3 Pseudopod formation changes before and after RNAi

Cell lines	Pseudopods before RNAi (/cell)	Pseudopods after RNAi (/cell)	Statistic analysis ($n = 5$)
SF7721	20.8 ± 3.0	13.2 ± 2.4	$t = 4.95$, $p < 0.01$
MHCC97-H	18.4 ± 2.7	14.0 ± 2.9	$t = 5.88$, $p < 0.01$
MHCC-1	22.6 ± 3.5	13.3 ± 1.9	$t = 5.56$, $p < 0.01$
$HepG_2$	31.0 ± 2.9	17.8 ± 2.3	$t = 5.71$, $p < 0.01$

Table 4 Comparison of cells transferring the artificial basal membrane

Cell lines	Transferring cells before RNAi	Transferring cells after RNAi	Statistics analysis ($n = 8$)
SF7721	49.9 ± 7.7	31.9 ± 5.2	$t = 7.12$, $p < 0.01$
MHCC97-H	58.5 ± 4.2	33.0 ± 3.3	$t = 20.3$, $p < 0.01$
MHCC-1	57.6 ± 6.1	28.3 ± 3.4	$t = 11.1$, $p < 0.01$
$HepG_2$	37.3 ± 3.0	25.3 ± 2.3	$t = 9.57$, $p < 0.01$

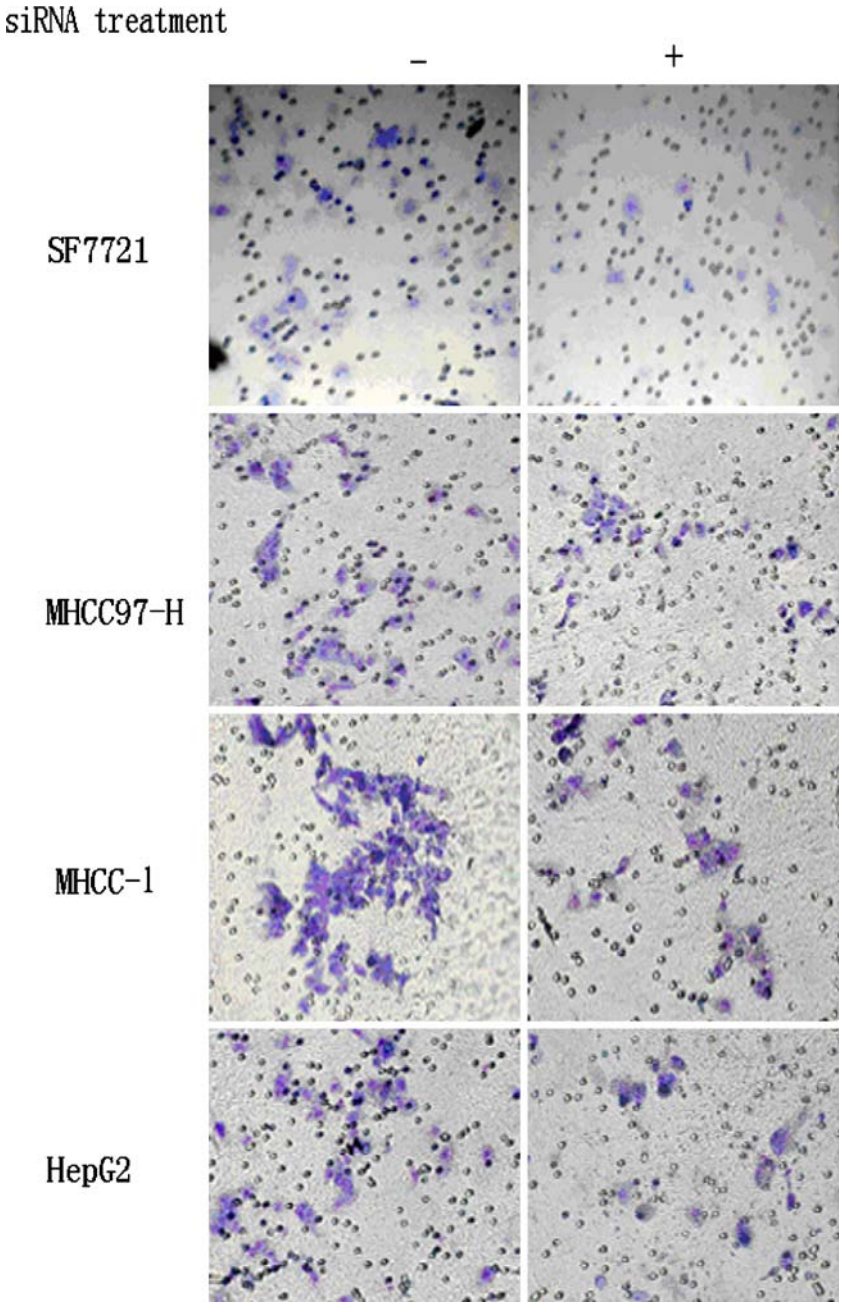

Fig. 10 Comparison of cells transferring the artificial basal membrane. The cells transferring membrane were significantly decreased after RNAi in all the hepatocellular carcinoma cell lines. It was suggested that the cancer cell mobility is decreased with low ezrin protein level (SF7721: $t = 7.12$, $p < 0.01$; MHCC97-H: $t = 20.3$, $p < 0.01$; MHCC-1: $t = 11.1$, $p < 0.01$; $HepG_2$: $t = 9.57$, $p < 0.01$)

and $HepG_2$ in the third day, respectively (Fig. 5). Down-regulation of ezrin protein occurred later than that in mRNA level, which occurred in the second day in RNAi-transfected SF7721 and in the third day in other cell lines. The maximum protein down-regulation rates of the four tested cell lines were all more than 70% (Fig. 6). In detail, about 85% ezrin appeared to be down-regulated in the second and third day after ezrin-siRNA4 transfection in SF7721, whereas 74% was down-regulated in $HepG_2$ in the fourth day after transfection, 80 and 95% were observed to be down-regulated in siRNA-transfected MHCC97-H, MHCC-1 in the fourth and fifth days, respectively (Fig. 6).

The effect of ezrin down-regulation on cell proliferation

We tested the cell proliferation changes by MTT assay. According to the growth curves of the four cell lines, we discovered that the proliferation of cancer cells was significantly suppressed by down-regulation of ezrin protein (Fig. 7, SF7721: $t = 3.2$; $p < 0.05$; MHCC97-H:

$t = 6.297$, $p < 0.01$; $HepG_2$: $t = 3.985$, $p < 0.01$; MHCC-1: $t = 5.856$, $p < 0.01$, $n = 10$).

The effect of ezrin down-regulation on cell cycles and apoptosis

We transfected ezrin-siRNA4 into four cell lines as described above and collected the cells in the day with maximum down-regulation rates for cell-cycle analysis. Using flow cytometer, we demonstrated that G2/M phase cells decreased dramatically in all tested cell lines after RNAi transfection. In detail, the proportions of G2/M cells decreased from 24.93 to 13.92% in MHCC-97H, decreased from 7.73 to 4.24% in $HepG_2$, decreased from 19.30 to 3.20% in MHCC-1, and decreased from 28.07 to 23.53% in SF7721. Although cells in G1 phase increased from 58.43 to 66.14% and from 62.44 to 66.54% in RNAi-transfected MHCC-1 and SF7721, respectively (Fig. 8), no apoptotic cells were observed in siRNA-transfected cells. Our results implicated that ezrin-siRNA may inhibit cell proliferation by interfering cell mitosis and cell-cycle transition.

The effect of ezrin down-regulation on pseudopods formation

Because the formation of pseudopods of cells are response to cell mobility and tumor metastasis, we compared the effects of ezrin down-regulation on pseudopods formation in ezrin-siRNA4-transfected tumor cells with scramble-transfected control by scanning electron microscopy. After attachment of the cells on cover slides, we count the number of pseudopods in five tested cells under 2,000 × magnified vision. The average numbers of pseudopods per cell were listed in Table 3. Totally, the average number of pseudopods decreased in ezrin down-regulated cells (SF7721: $t = 4.95$, $p < 0.01$; MHCC97-H: $t = 5.88$, $p < 0.01$; MHCC-1: $t = 5.56$, $p < 0.01$; HepG2: $t = 5.71$, $p < 0.01$, $n = 5$). Furthermore, the pseudopods of cells after RNAi transfection were shorter and thinner than that of controls in morphology (Fig. 9).

The effect of ezrin down-regulation on tumor cell invasiveness in vitro

Transwell assays were used to investigate the alteration of cancer cell invasiveness after RNAi by staining cells with Giemsa and counting cells with q 20× objective microscope. In all experiments, we usually count cells at least eight fields per membrane. The data were listed in Table 4. Down-regulation of ezrin expression can also inhibit the mobility and the invasiveness of hepatocellular carcinoma cell lines in vitro (Fig. 10; SF7721: $t = 7.12$, $p < 0.01$; MHCC97-H: $t = 20.3$, $p < 0.01$; MHCC-1: $t = 11.1$, $p < 0.01$; HepG2: $t = 9.57$, $p < 0.01$, $n = 8$).

Discussion

Increase in cell mobility is the common feature of tumor metastasis. To migrate, cells use dynamic rearrangements of actin cytoskeleton for the formation of protrusive structures and for the generation of intracellular forces that lead to net cell translocation. In addition, actin-based cell mobility relies not only on actin itself, but also on numerous actin interacting proteins that drive the dynamics of the actin system and govern its spatial organization. Ezrin, an actin-binding protein, plays a role in the formation of microvilli, cell adhesion sites, lamellipodia formation, and contractile rings during cytokinesis (Pawlak and Helfman 2000). Ezrin protein is involved in the interaction of the cell cytoskeleton with the plasma membrane, during signal transduction and growth control (Andreoli et al. 1994), and plays a key role in the control of cell morphology (Hiscox and Jiang 1999). Ezrin is a substrate for the tyrosine kinase HGF/SF receptor both in vitro and in vivo. After phosphorylated at threonine in C-terminal domain by Rho kinase (Tran et al. 2000; Matsui et al. 1998), or at tyrosine in N-terminal domain by receptor tyrosine kinases via epidermal growth factor receptor and c-met signaling pathway (Krieg and Hunter 1992; Crepaldi et al. 1997), ezrin will promote cytoskeletal reorganization and cause subsequent morphogenetic alteration. The truncated form ezrin, however, impairs the cells morphogenic and motogenic response to HGF/SF, suggesting a dominant-negative mechanism of action. So ezrin is thought to function as general cross-linkers between plasma membranes and actin filaments in the cytoplasm (Yonemura et al. 2002).

Some studies have implicated that ezrin proteins play an important role in cell transformation. They have been found to be over-expressed in metastatic cell lines (Small 1994), resulting increasing invasion ability in endometrial cancer cells (Small et al. 1998). Over-expression of ezrin in many cultured cells causes cell transformation and is associated with cell proliferation (Small et al. 2002). Although many types of tumors express ezrin, little is known about its biological functions. Therefore, we screened the differential protein expression of ezrin in six hepatocellular carcinoma cell lines by immunofluorescence, RT-PCR, and western blot. The results tell us that ezrin over-expresses in the cell lines with high metastasis potential and F-actin

often co-expresses with ezrin, which imply that ezrin might increase the cell mobility via altering actin expression and organization in hepatocellular carcinoma cells. An increasing expression of γ-actin but not β-actin was also observed in our experiments. The role of γ-actin on tumor proliferation and invasiveness needs to be further studied.

RNAi is an evolutionary conserved process in which recognition of dsRNA ultimately leads to post-transcriptional suppression of gene expression. This natural response has been developed into a powerful tool for the investigation of gene function. So we use siRNA to down-regulate ezrin expression and compare the proliferation and invasiveness before and after RNAi. The outcomes demonstrated cell proliferation significantly slow down in lower ezrin expressed tumor cells. In vitro mobility and invasion assay also gain anticipating results. Lamellipodia and filopodia (Lamb et al. 1997; Kaul et al. 1996) are two cellular features formed by actin filament associated with cell migration. So we observed pseudopods formation under electron microscopy. Lower ezrin expression level can significantly inhibit pseudopods formation, suggesting the reduction of cell mobility and invasion. Transwell assay further proved our previous results. This study had also proved that ezrin is a crucial molecule in the dissemination of two pediatric tumors rhabdomyosarcoma (Yu et al. 2004) and osteosarcoma (Khanna et al. 2004). Transfection of full-length ezrin constructs into low-metastatic cell lines dramatically increased the ability of these cell lines to form macroscopic pulmonary lesions in experimental metastasis assays, demonstrating that ezrin over-expression is sufficient to confer metastatic capacity. More importantly, using dominant-negative mutants, antisense RNA, or RNA interference (RNAi), two different groups demonstrated that ezrin over-expression is sufficient and necessary for metastatic progression, at least in this system (Yu et al. 2004; Khanna et al. 2004). Other studies showed ezrin also participated in other cancer type metastasis (Chen et al. 2001; Shen et al. 2003; Masahide et al. 2000; Harrision et al. 2002). Our outcomes were in accordance to these studies and gain the conclusion that ezrin is necessary in the process of hepatocellular carcinoma cell growth, migration, and invasiveness.

Our preliminary results in vitro study about ezrin in hepatocellular carcinoma growth and invasiveness had paved the way for the further clinical studies to evaluate biological therapeutical effects of radical therapy in preventing tumor relapse and invasion in hepatocellular carcinoma. However, in vivo study about ezrin function system is still needed to validate its role in tumor dissemination and metastasis.

References

Andreoli C, Martin M, Le Borgne R, Reggio H, Mangeat P (1994). Ezrin has properties to self-associate at the plasma membrane. J Cell Sci 107(9):2509–2521

Bretscher A, Edwards K, Fehon RG (2002) ERM proteins and merlin: integrators at the cell cortex. Nat Rev Mol Cell Biol 3:586–599

Chen ZC, Fadiel A, Feng YJ, Ohtani K, Rutherford T, Naftolin F (2001) Ovarian epithelial carcinoma tyrosine phosphorylation, cell proliferation, and ezrin translocation are stimulated by interleukin 1 alpha and epidermal growth factor. Cancer 92:3068–3075

Crepaldi T, Gautreau A, Comoglio PM, Louvard D, Arpin M (1997) Ezrin is an effector of hepatocyte growth factor-mediated migration and morphogenesis in epithelial cell. J Cell Biol 138(2):423–434

Harrision GM, Davies G, Martin TA (2002) Distribution and expression of CD44 isoforms and ezrin during prostate cancer–endothelium interaction. Int J Oncol 21:935–940

Hiscox S, Jiang WG (1999) Ezrin regulates cell–cell and cell–matrix adhesion: a possible role with E-cadherin/beta-catenin. J Cell Sci 112(18):3081–3090

Kaul SC, Mitsui Y, Komatsu Y, Reddel RR, Wadhwa R (1996) A highly expressed 81 kDa protein in immortalized mouse fibroblast: its proliferative function and identity with ezrin. Oncogene 13(6):1231–1237

Khanna C, Wan X, Bose S, Cassaday R, Olomu O, Mendoza A, Yeung C, Gorlick R, Hewitt SM, Helman LJ (2004) The membrane-cytoskeleton linker ezrin is necessary for osteosarcoma metastasis. Nat Med 10(2):182–186

Krieg J, Hunter T (1992) Identification of the two major epidermal growth factor-induced tyrosine phosphorylation sites in the microvillar core protein ezrin. J Biol Chem 267:19258–19265

Lamb RF, Ozanne BW, Roy C, McGarry L, Stipp C, Mangeat P, Jay DG (1997) Essential functions of ezrin in maintenance of cell shape and lamellipodial extension in normal and transformed fibroblasts. Curr Biol 7(9):682–688

Masahide T, Toshiro N, Yukihito S (2000) Altered expression of the ERM proteins in lung adenocarcinoma. US Can Acad Pathol 80(11):1643–1650

Matsui T, Maeda M, Doi Y, Yonemura S, Amano M, Kaibuchi K, Tsukita S, Tsukita S (1998) Rho-kinase phosphorylates COOH-terminal threonines of ezrin/radixin/moesin (ERM) proteins and regulates their head-to-tail association. J Cell Biol 140:647–657

Nguyen R, Reczek D, Bretscher A (2001) Hierarchy of merlin and ezrin N and C-terminal domain interactions in homo and heterotypic associations and their relationship to binding of scaffolding proteins EBP50 and E3KARP. J Biol Chem 276:7621–7629

Ohtani K, Sakamoto H, Rutherford T, Chen Z, Satoh K, Naftolin F (1999) Ezrin, a membrane-cytoskeletal linking protein, is involved in the process of invasion of endometrial cancer cells. Cancer Lett 147(1/2):31–38

Pawlak G, Helfman DM (2000) Cytoskeletal changes in cell transformation and tumorigenesis. Curr Opin Genet Dev 11(1):41–47

Sainio M, Zhao F, Heiska L, Turunen O, den Bakker M, Zwarthoff E, Lutchman M, Rouleau GA, Jaaskelainen J, Vaheri A, Carpen O (1997) Neurofibromatosis 2 tumour suppressor protein colocalizes with ezrin and CD44 and associates with actin-containing cytoskeleton. J Cell Sci 110:2249–2260

Shen ZY, Xu LY, Chen MH, Li EM, Li JT, Wu XY, Zeng Y, Xu LY, Chen MH, et al. (2003) Upregulated expression of ezrin and invasive phenotype in malignantly transformed

esophageal epithelial cells. World J Gastroenterol 9(6):1182–1186

Small JV (1994) Lamellipodia architecture: actin filament turnover and the lateral flow of actin filaments during motility. Semin Cell Biol 5:157–163

Small JV, Rottner K, Kaverina I, Anderson KI (1998) Assembling an actin cytoskeleton for cell attachment and movement. Biochim Biophys Acta 1404:271–281

Small JV, Stradal T, Vignal E, Rottner K (2002) The lamellipodium: where motility begins. Trends Cell Biol 12:112–120

Tran Quang C, Gautreau A, Arpin M, Treisman R (2000) Ezrin function is required for ROCK-mediated fibroblast transformation by the net and dbl oncogenes. EMBO J 19:4565–4576

Xie Q, Liu KD, Hu MY, Zhou K (2001) SF/HCF-c-met autocrine and paracrine promote metastasis in hepatocellular carcinoma. World J Gastroenterol 7:816–820

Yonemura S, Tsukita S, Tsukita S (1999) Direct involvement of ezrin/radixin/moesin (ERM)-binding membrane proteins in the organization of microvilli in collaboration with activated ERM proteins. J Cell Biol 145(7):1497–1509

Yonemura S, Matsui T, Tsukita S (2002) Rho-dependent and -independent activation mechanisms of ezrin/radixin/moesin proteins: an essential role for polyphosphoinositides in vivo. J Cell Sci 115:2569–2580

Yu Y, Khan J, Khanna C, Helman L, Meltzer PS, Merlino G (2004) Expression profiling identifies the cytoskeletal organizer ezrin and the developmental homeoprotein Six-1 as key metastasic regulators. Nat Med 10(2):175–181